SUPPLEMENTARY INFORMATION

DFT insights into structural effects of Ni-Cu/CeO_2 catalysts for CO selective reaction towards Water-Gas Shift

Agustín Salcedo[ab], *Beatriz Irigoyen*[ab*]

[a]Universidad de Buenos Aires. Facultad de Ingeniería. Departamento de Ingeniería Química. Pabellón de Industrias, Ciudad Universitaria, C1428EGA Buenos Aires, Argentina.

[b]CONICET–Universidad de Buenos Aires. Instituto de Tecnologías del Hidrógeno y Energías Sostenibles (ITHES). Pabellón de Industrias, Ciudad Universitaria, C1428EGA Buenos Aires, Argentina.

Corresponding Author

*beatriz@di.fcen.uba.ar

1. CeO_2(111) slab

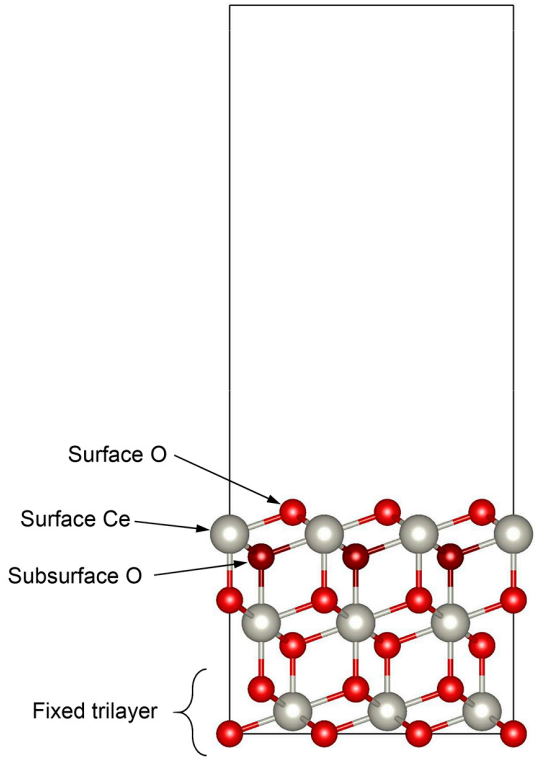

Figure S1. CeO_2(111) slab.

2. Supported and gas-phase clusters

Table S1. Calculated total magnetic moment (M_{tot}), binding energies (E_{bin}), adsorption energies (E_{ads}) and excess energies (E_{exc}) of $Ni_{4-x}Cu_x$ clusters. "t" and "r" indicate tetrahedral and rhombohedral clusters respectively.

Cluster	Gas-phase						Supported					
	M_{tot} (μB)		E_{bin} (eV/at)		E_{exc} (eV)		M_{tot} (μB)		E_{ads} (eV)		E_{exc} (eV)	
	t	r	t	r	t	r	t	r	t	r	t	r
Ni_4	4	4	2.51	2.48	-	-	4	4	−6.79	−6.66	-	-
Ni_3Cu_1	1	3	2.18	2.25	0.41	0.13	3	3	−6.96	−6.54	−0.35	0.08
Ni_2Cu_2	0	2	1.89	2.01	0.66	0.17	2	2	−6.33	−6.19	0.01	0.14
Ni_1Cu_3	0	1	1.61	1.76	0.87	0.27	1	1	−5.89	−5.94	0.23	0.18
Cu_4	-	0	-	1.60	-	-	0	0	−5.54	−5.32	-	-

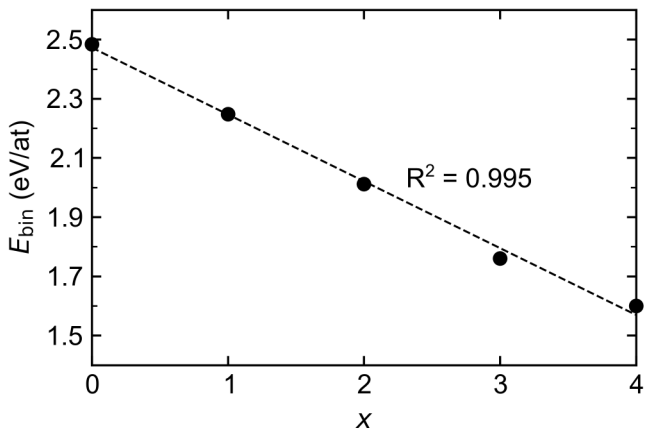

Figure S2. Binding energies for the most stable (rhombohedral) isomers as a function of the number of Cu atoms in the cluster (x). Linear fitting is shown as a dashed line.

3. Bader charge analysis

Table S2. Bader charge difference (Δq in |e|) for Ni and Cu atoms of the pyramidal $Ni_{4-x}Cu_x$ clusters upon adsorption on the $CeO_2(111)$ surface, as well as the reduced Ce ions.

Cluster	Apex	Base atoms	Ce ions
Ni_4	0.033	−0.328, −0.332, −0.322	0.302, 0.304
Ni_3Cu_1	0.020	−0.330, −0.321, −0.317	0.302, 0.302
Ni_2Cu_2	0.017	−0.342, −0.324, −0.300	0.302, 0.302
Ni_1Cu_3	0.002	−0.314, −0.338, −0.332	0.301, 0.299
Cu_4	−0.010	−0.317, −0.327, −0.345	0.326, 0.325

Table S3. Vacancy formation energies and Bader charge differences for Ni and Cu atoms in pyramidal $Ni_{4-x}Cu_x$ clusters supported on an O-defective and a hydroxylated $CeO_2(111)$ surface, compared to the clusters adsorbed on the clean stoichiometric surface.

Cluster	Δq (|e|) O-defective					Δq (|e|) Hydroxylated			
	E_{vac} (eV)	Apex	Base atoms			Apex	Base atoms		
Ni_4	1.96	0.014	−0.011	0.018	0.022	0.020	0.008	0.010	0.035
Ni_3Cu_1	1.96	0.007	0.021	−0.009	0.019	0.017	0.031	0.018	0.001
Ni_2Cu_2	1.96	0.011	0.004	0.016	0.010	0.020	0.011	0.019	0.003
Ni_1Cu_3	1.97	0.011	0.015	0.002	0.015	0.020	0.015	0.006	0.012
Cu_4	1.98	0.016	−0.004	0.012	0.014	0.023	−0.006	0.014	0.025

Table S4. Bader charge difference (Δq in |e|) for C, O, Ni and Cu upon on-top adsorption of CO on the pyramidal $Ni_{4-x}Cu_x$ clusters supported on $CeO_2(111)$.

Cluster	C	O	CO	Apex	Base atoms		
Ni_4	0.146	0.058	0.204	−0.215	0.067	0.010	−0.034
Ni_3Cu_1	0.039	0.078	0.117	−0.225	0.058	0.016	0.027
Ni_2Cu_2	0.039	0.082	0.121	−0.238	0.034	0.039	0.039
Ni_1Cu_3	0.045	0.035	0.079	−0.199	0.020	0.047	0.045
Cu_4	0.048	0.007	0.055	−0.190	0.037	0.036	0.042

4. Density of states

Table S5. Integration of the density of states projected onto the d-states of Ni and Cu atoms in the supported $Ni_{4-x}Cu_x$ clusters, in the range of 0 to 8.0 eV (empty states).

Site	Band	$Cu_4/CeO_2(111)$	$Ni_4/CeO_2(111)$	$Ni_3Cu_1/CeO_2(111)$
Base (3 ions)	dxy	0.224	0.860	0.829
	dyz	0.322	0.746	0.636
	dz^2	0.303	1.100	1.187
	dxz	0.335	0.653	0.656
	dx^2-y^2	0.229	0.833	0.812
	dtotal	1.414	4.192	4.121
	s	0.591	0.472	0.482
Apex (1 ion)	dxy	0.040	0.133	0.040
	dyz	0.087	0.358	0.092
	dz^2	0.053	0.084	0.054
	dxz	0.087	0.281	0.093
	dx^2-y^2	0.040	0.330	0.040
	dtotal	0.306	1.186	0.319
	s	0.237	0.197	0.214

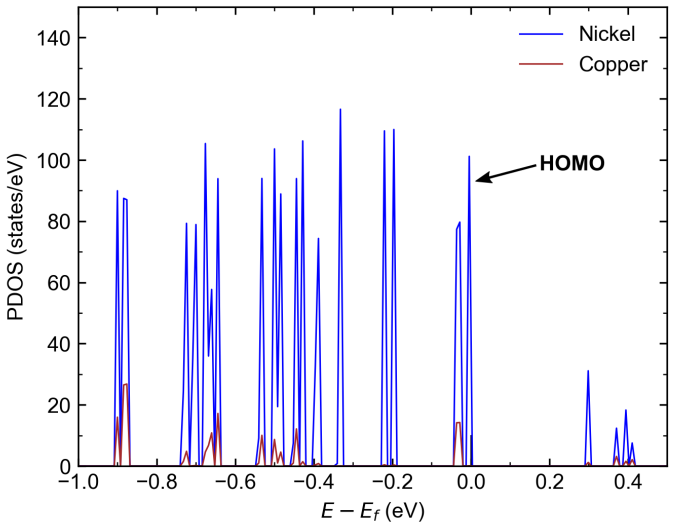

Figure S3. Projected density of states (PDOS) onto the d-states of Ni and Cu atoms in the Ni_3Cu_1 gas-phase cluster. The energy is referred to the Fermi level (E_f). The highest occupied molecular orbital is indicated by an arrow.

5. CO adsorption on supported $Ni_{4-x}Cu_x$ clusters

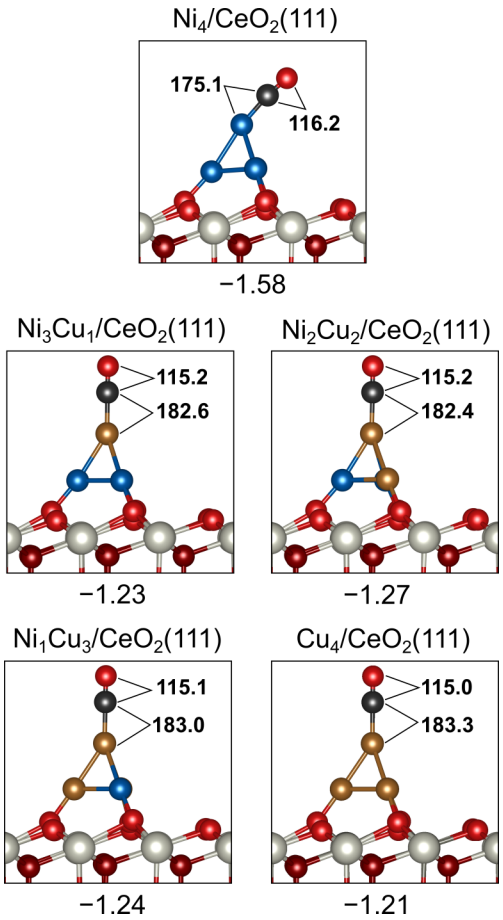

Figure S4. Geometric structures, adsorption energies (eV) and distances (pm), for CO adsorbed on the apex atom of supported $Ni_{4-x}Cu_x$ clusters. Carbon is represented in black. Nickel and copper in blue and brown, respectively. Ce cations in light gray, and surface/subsurface oxygen in light/dark red.

6. d-band center analysis

Table S6. d-band center energy (eV) of tetrahedral $Ni_{4-x}Cu_x$ clusters supported on $CeO_2(111)$, evaluated using both the classic Hammer-Nørskov method (HN) and the Bhattacharjee-Waghmare-Lee correction (BWL). The average d-band center ($\bar{\varepsilon}_d$) of $Ni_{4-x}Cu_x$ clusters as well as the d-band center of their apex atoms ($\varepsilon_d^{\text{apex}}$) are reported.

x	HN		BWL	
	$\bar{\varepsilon}_d$	$\varepsilon_d^{\text{apex}}$	$\bar{\varepsilon}_d$	$\varepsilon_d^{\text{apex}}$
0	−1.10	−0.99	−1.21	−1.09
1	−1.34	−1.80	−1.42	−1.80
2	−1.43	−1.68	−1.48	−1.68
3	−1.66	−1.93	−1.68	−1.93
4	−1.74	−1.83	−1.74	−1.83

7. Calculation of transition states

Transition state (TS) structures were located using the climbing image nudged elastic band method (CI-NEB) with a spring force of 5 eV/Å. A 6-layer (2 TL) p(3×3) slab was used in these calculations. Full relaxation of atomic coordinates was allowed for the ions located in the three uppermost layers, keeping the bottom layers fixed. Forces were converged to 0.15 eV/Å. Vibrational frequencies were calculated to verify the transition states, using finite differences as implemented in VASP, with atomic displacements of ±0.015 Å.

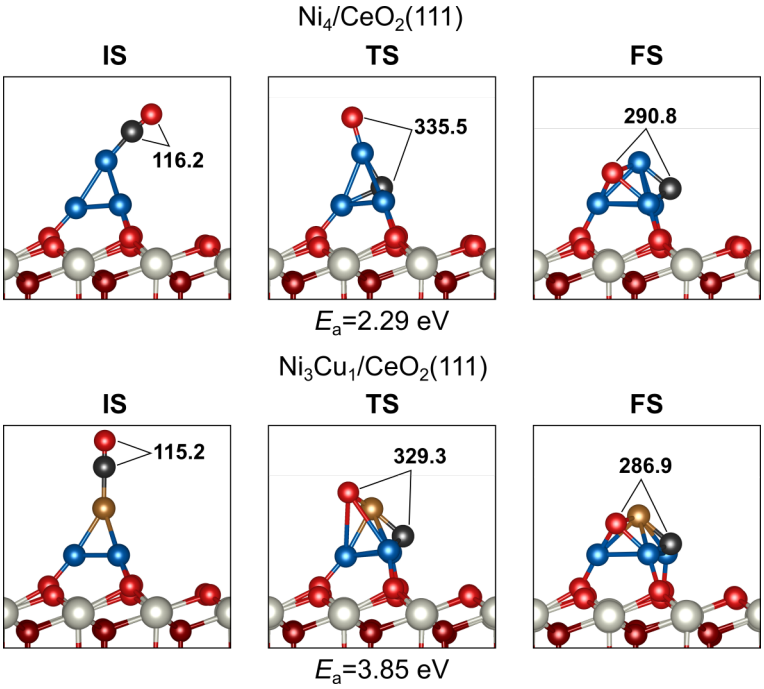

Figure S5. Initial state (IS), transition state (TS), final state (FS) and distances (pm), for CO dissociation on the Ni_4 and Ni_3Cu_1 clusters supported on $CeO_2(111)$. Carbon is represented in black. Nickel and copper in blue and brown, respectively. Ce cations in light gray, and surface/subsurface oxygen in light/dark red.